IJST, Transactions of Mechanical Engineering, Vol. 39, No. M2, pp 427-436
Printed in The Islamic Republic of Iran, 2015

PARAMETRIC STUDY FOR RESIDUAL STRESSES AND DEFORMATIONS IN WELDED PIPE-FLANGE JOINTS*

M. ABID[1**], H. ABDUL WAJID[2] AND S. ULLAH[3]

[1]Interdisciplinary Research Center, COMSATS Institute of Information Technology, Wah Cantt, Pakistan
Email: drabid@ciitwah.edu.pk
[2]Dept. of Mathematics, COMSATS Institute of Information Technology, Lahore, Pakistan
[2]Dept. of Electrical Engineering, Faculty of Engineering, Islamic University Medina, KSA
[3]Faculty of Mechanical Engineering, GIK Institute of Engineering Sciences and Technology, Topi, Pakistan

Abstract– Welding produces residual stresses and distortion, having detrimental effect on structure integrity and service performance of the welded pipe joints. This paper investigates residual stresses and distortion during Gas Metal Arc Welding (GMAW) of pipes of schedule 40 and 60, nominal diameter 100mm and 200mm and thickness 8mm and 10mm with ANSI flanges of class 300#. Welding parameters including voltage, current and heat input are varied to find the optimized set to control stresses and deformations. Stress variation on the flange side is observed prominent compared to the pipe side due to its dimensional variation. Axial flange displacement along 360 degrees is also concluded obvious, hence effecting sealing performance of the gasketed flanged pipe joints.

Keywords– Welding and geometric parameters, residual stresses, deformations, welded pipe-flange joints

1. INTRODUCTION

Electric fusion process is reported in 1782 in Germany by Lichtenberg [1], and electric arc welding process is reported in the nineteenth century. Vaidyanathan *et al* [2] provided a methodology for the determination of residual stresses in thin walled cylindrical shells. Rybicki *et al* [3-6] performed two dimensional finite element analyses (FEA) for a variety of the welding conditions, including multi-pass weld, partial penetration of weld and different filler and base materials. Jonsson *et al* performed experimental and numerical (2D and 3D) studies work in order to determine transient and residual stresses [7-8]. Lindgren *et al* performed 3D FEA using shell elements to study deformation and stresses in welded thin walled pipes [9]. Rosenthal [10] presented heat source distribution for thin plates using temperature dependent material model taken from Karlsson *et al* [11, 12]. Karlsson and Josefson concluded that 2D model provides reasonable results for residual stresses, whereas 3D model is necessary for transient stresses for welded pipes [7, 9]. The effect of welding distortions and residual stresses on load carrying capacity of the pipe was studied by Troive *et al.* who performed 3D FEA analysis for thin walled pipe with thermo-elasto-plastic shell elements and discussed the effect of size of pipe and flange on residual stresses [13-15]. Teng and Chang [16] using axi-symmetric FE model for pipe-pipe joint, studied the effect of pipe diameter and wall thickness on residual stresses and results were found in agreement with the Rybicki *et al* [17-18]. Abid and Siddique [19-31] have performed detailed parametric welding simulations of pipe-flange joints and have studied the effect of welding, geometric and other parameters on residual stresses and welding distortion. They concluded that the effect of decreasing current is almost similar to the increasing welding speed, at least for the range of parameters used in their study. They concluded that the main factor is the heat input per unit length of weldment, which has positive effect on

*Received by the editors October 27, 2014; Accepted May 13, 2015.
**Corresponding author

the magnitude of the residual stresses and zone of influence. Pipe diameter has significant effect on the magnitude of residual stresses as well as on the zone of influence. Pipe wall thickness has negative effect on the magnitude of the residual stresses because pipe of smaller wall thickness has low stiffness and is more prone to the radial shrinkage resulting bending stresses. They concluded that any change in tack weld location alters the axial displacement and tilt of the flange face. Regarding root gap opening it is found that root gap should be a minimum, just to meet the need of weld penetration. Large root gap increases lateral shrinkage and results in higher axial displacement and flange face tilt. Structural constraints were modeled representing welding fixture in girth welding of pipe-flange joints and to determine the effect of different constraints with the objective to minimize flange deformations. Abid and Jawad [32-35] have performed detailed three dimensional finite element analyses for multi pass welding. They have described the details of welding sequence; inter pass cooling and effect of different parameters on residual stresses and deformations. FE methodology presented in the present study can be helpful for developing welding procedures for a range of pipe flange welded joints for controlled residual stresses and deformations for optimized performance during bolt up and operating conditions.

2. WELDING PARAMETERS

Temperature dependent material properties of low carbon steel with chemical composition 0.18%C, 1.3%Mn, 0.3%Si, 0.3%Cr, 0.4%Cu are used [9, 36]. Change in microstructure and fluid flow of a material is not taken into account, and effect of welding on mechanical property is considered only. Goldak *et al.* [37-38] double ellipsoidal heat source model is used as this has excellent characteristics of power density distribution control in the weld pool and HAZ Conductivity of 120W/m°C in the liquid range for low carbon steel is taken from Goldak [37-38]. In order to model fluid flow (stirring) effect on the thermal field, thermal conductivity is given an artificial rise to 230KJ/mK at solidus temperature [39]. Temperature dependent specific heat value used in [40] is taken and latent heat of fusion of 260KJ/kg is specified for low carbon steel. Young's modulus of 12.4GPa is used, however, even lower value of 1GPa is also reported in [40]. The values for both the bulk modulus and Poisson's ratio are taken constant after 1200°C.

3. HEAT SOURCE MODELING

Goldak *et al.* [37-38] double ellipsoidal heat source model is used in the present work, as this has excellent characteristics of power density distribution control in the weld pool and HAZ. The heat source that was initially presented for plate welding is slightly modified in order to make it suitable for circumferential or hoop welding. For this purpose, the arbitrary candidate spatial location within the heat source is calculated by using cylindrical coordinate system. Geometry of the double ellipsoidal heat source is shown in Fig. 1a and dimension of double ellipsoidal heat source verified using MATLAB software shown in Fig. 1b.

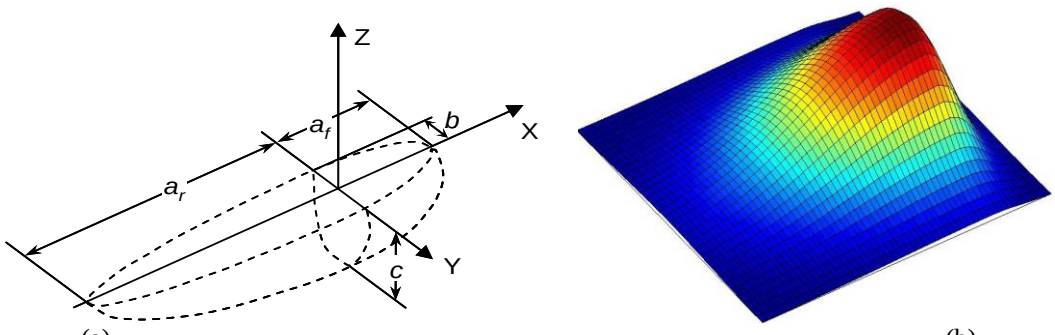

(a) (b)

Fig. 1. (a) Geometry of double ellipsoidal heat source, (b) Power density distributions by using double ellipsoidal heat source model

4. FINITE ELEMENT MODELING, MESHING AND BOUNDARY CONDITIONS

Weld neck flanges of ANSI Class # 300 [41] are analyzed with pipe of length 200mm of schedule 40 and 60 to observe residual stresses and displacement behavior during welding. Details of welding and geometrical parameters and case studies performed are given in Table 1 and Table 2 respectively. Single pass GMAW simulation is performed using root gap of 1.2mm, element length along radial and circumferential direction of 2mm and 9.44mm respectively, along axial direction in melted and heat effected zone of 1.42mm.Weld tack location is at 90 and 270 degrees from weld start position as suggested by Abid et al. [19-22] and each tack length is 18.9 mm with thickness of 4mm. Tack welds also act as the boundary condition and restrain free body motion of the flange. Consequently, the stiffness of the tack welds is reduced to a very small value and permits unrestrained motion of the flange during the thermal cycle. For structural boundary condition all the nodes at the far end are constrained to model pipe effect.3D FEA takes about 113 sec. to complete circumferential weld with the welding sequence divided into 120 equally spaced solution steps of 0.941sec. Each 3D model with applied constraints and bolt holes is shown in Fig. 2a and tack weld position is shown in Fig. 2b.

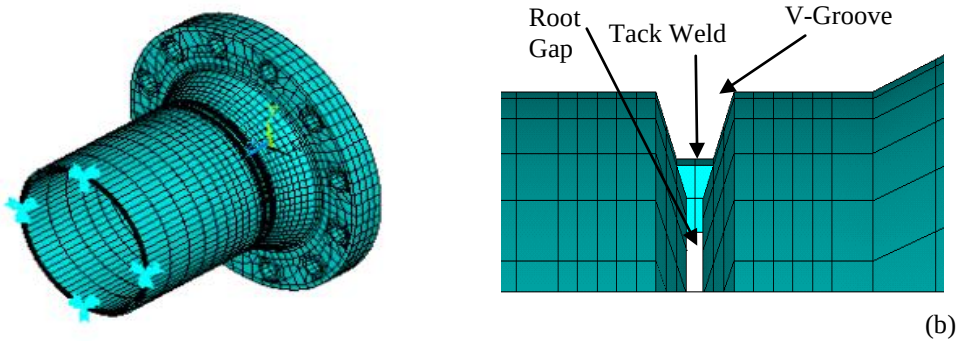

Fig. 2. (a) 3D FE model of pipe-flange joint, (b) Tack weld position

Using finite element analysis software ANSYS [42], quite element technique is used where complete FE model, including all the elements and nodes of base metal and filler metal is developed at the start. The filler metal elements are deactivated by assigning them a very low thermal conductivity (in thermal analysis) and very low stiffness (in structural analysis). The elements of specific weld bead are reactivated by "element birth" option at the start of the respective weld bead or when they come under the influence of the welding torch. The material properties of reactivated elements are instated at the time of activation [43]. During fusion welding process, a very concentrated heat source is applied hence characteristics of heat source are determined by its intensity. Therefore, based on the data given in [44], heat intensity of 80W/mm^2 and maximum torch speed of up to 7mm/sec is selected.

Table 1. Welding and geometrical parameters

Case No.	Arc voltage (Volt)	Welding current (Amp)	Arc efficiency (%)	Surface area (mm^2)	Welding speed (mm/sec)	Nominal pipe dia. (mm)	Pipe sche-dule	Wall Thick-ness (mm)	Heat Intensity (W/mm^2)
C-1	25	315	85	90	6.00	200	40	8.0	87.5
C-2	25	315	85	90	6.25	200	40	8.0	87.5
C-3	25	315	85	90	6.50	200	40	8.0	87.5
C-4	25	300	85	90	6.25	200	40	8.0	83.3
C-5	25	330	85	90	6.25	200	40	8.0	91.6
C-6	25	330	85	90	6.25	200	60	10.0	91.6
C-7	25	315	85	90	6.25	100	40	8.0	87.5

Table 2. Case studies performed

Sr. No.	Parameter studied	Cases compared	Parameter range
1	Welding speed	C-1, C-2, C-3	6, 6.25 and 6.5 (mm/s)
2	Welding current	C-4, C-2, C-5	300, 315 and 330 (amp)
3	Pipe diameter	C-2, C-7	200, 100 (mm)
4	Thickness	C-5, C-6	8, 10, 12.6 (mm)

5. RESULTS AND DISCUSSION

a) *Effect of welding speed on axial and hoop residual stresses*

Case studies C-1, C-2 and C-3 are conducted at three different welding speeds (6, 6.25, 6.5mm/sec) keeping all other parameters constant. Almost similar residual hoop and axial residual stresses at all speeds are concluded due to the very small increase in welding speed [Figs. 3a-b]. Hoop stresses shift more towards flange side at outer diameter, whereas axial stresses shift towards flange side at both the inner and outer diameters. At inner diameter mostly tensile hoop stresses are observed at both the pipe and flange side up to 30mm from weld centerline; whereas at the outer diameter tensile stresses are observed only on the flange side up to 30 mm from weld centerline. Axial stresses are observed tensile and compressive at inside and outside diameters respectively on pipe side, whereas on flange side trends are reversed. This is concluded due to the thickness variations at pipe and flange sides. Figure 4 shows that as welding speed increases, axial displacement at flange inner and outer diameter increases from 90 degrees (first tack) to 300 degrees (approximately second tack) and decreases from 300degrees (second tack) to 90degrees (first tack). Weld start at zero degree and move toward first tack which is at 90degrees from weld start position and then to second tack which is 270 degrees away from weld starts position. Magnitude of axial displacement remains the same at weld start and end positions.

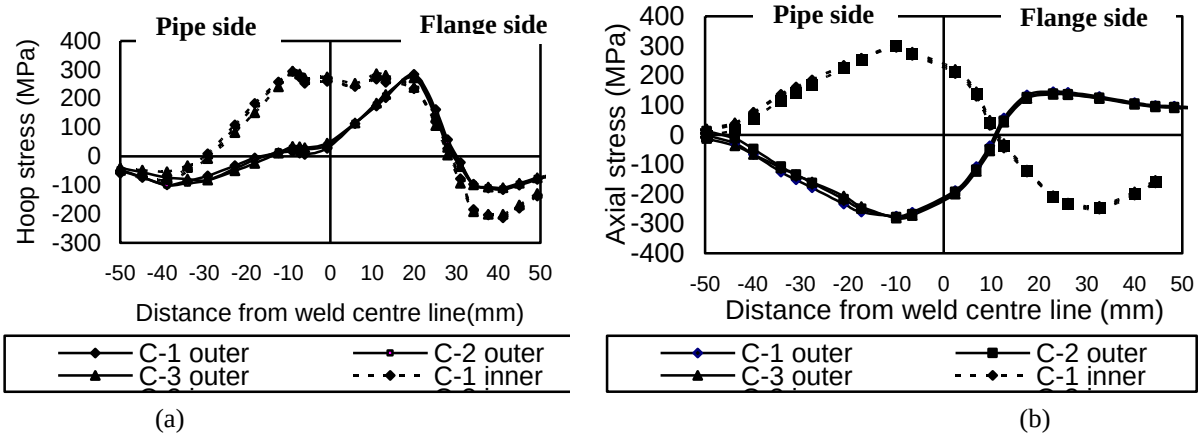

(a) (b)

Fig. 3. Residual stress variation at a section 180 degrees from weld start position: (a) Hoop, (b) Axial

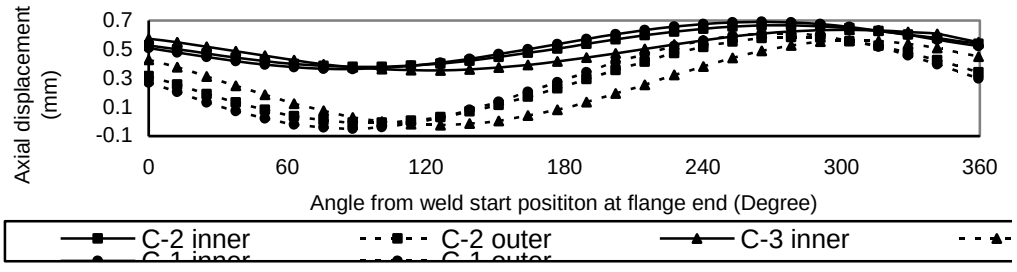

Fig. 4. Axial displacements along inner and outer diameter at flange end

b) Effect of welding current on axial and hoop residual stresses

Case studies C-2, C-4 and C-5 at three different welding currents 315, 300 and 330 ampere respectively are conducted keeping all other parameters constant. From the result of Fig. 5 it is concluded that increase in welding current has no significant effect on hoop and axial residual stresses. However, it is concluded that the zone of influence of axial and hoop stresses increases as welding current increases at both the inner and outer diameters of pipe and flanges. At outer diameter, hoop stresses shift toward flange side, whereas axial stress also has the shift at the inner and outer diameter. Figure 6, shows that as welding current increases, axial displacement at flange inner and outer diameter increases from 90 degrees (first tack) to 300 degrees (approximately second tack) and decreases from 300 degrees (second tack) to 90 degrees (first tack). Weld start at zero degree and move toward first tack which is at 90 degrees from weld start position and then to second tack which is 270 degrees away from weld start position. Magnitude of axial displacement remains the same at weld start and end position.

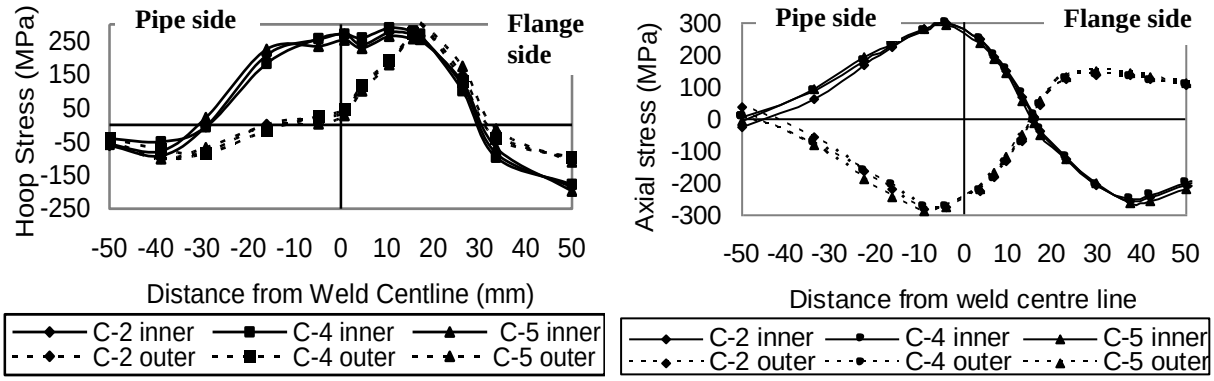

(a) (b)

Fig. 5. Residual stress variation at a section 180 degrees from weld start position: (a) Hoop, (b) Axial

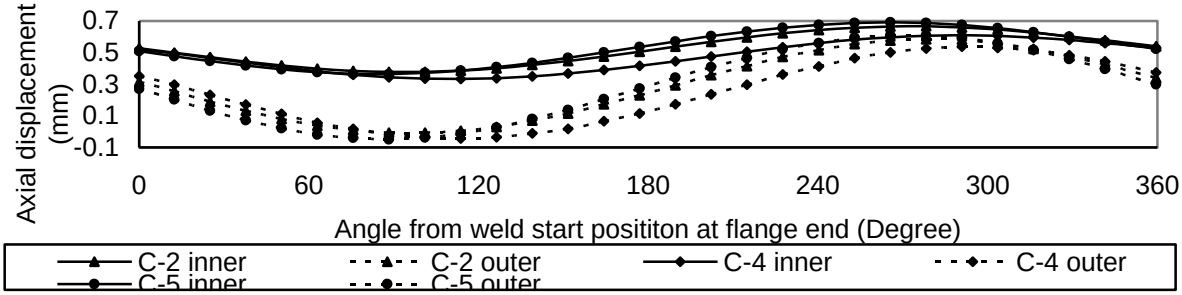

Fig. 6. Axial displacements along inner and outer circumference at flange end

c) Effect of pipe diameter on axial and hoop residual stresses

Case studies C-2 and C-7 are conducted for pipe diameter 200mm and 100mm respectively. It is concluded that as pipe diameter increases, magnitude of hoop and axial residual stress and their zone of influence increases at pipe and flange inner and outer diameter [Fig. 7]. At centerline residual stresses are observed maximum for larger diameter of pipe and flange. More axial displacement is observed for smaller pipe diameter with a very small variation at both the inner and outer diameters. For larger pipe diameter, more axial displacement is observed at outer diameter compared to the inner diameter. However, axial displacement remains the same at the weld start and end position for both the cases [Fig. 8].

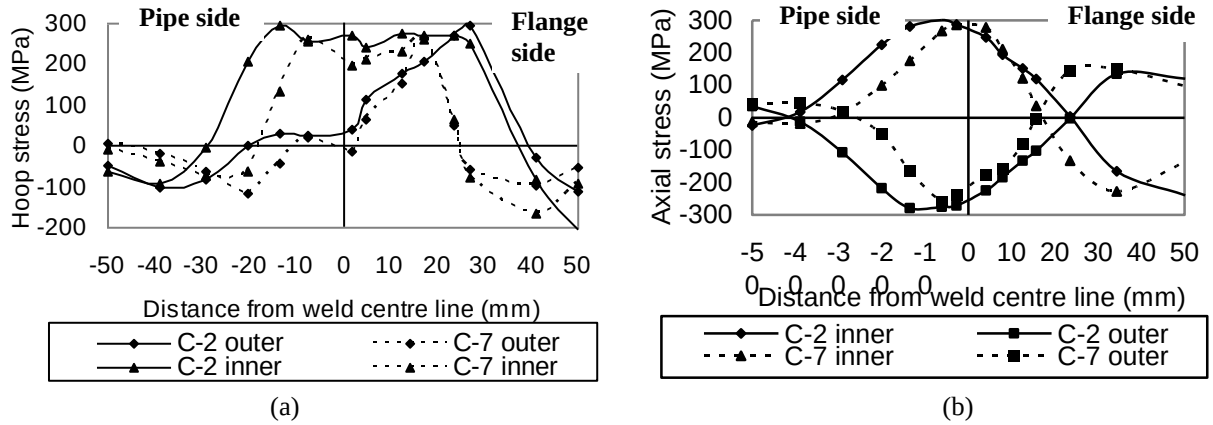

(a) (b)

Fig. 7. Residual stress variation at a section of 180 degrees from weld start position: (a) Hoop, (b) Axial

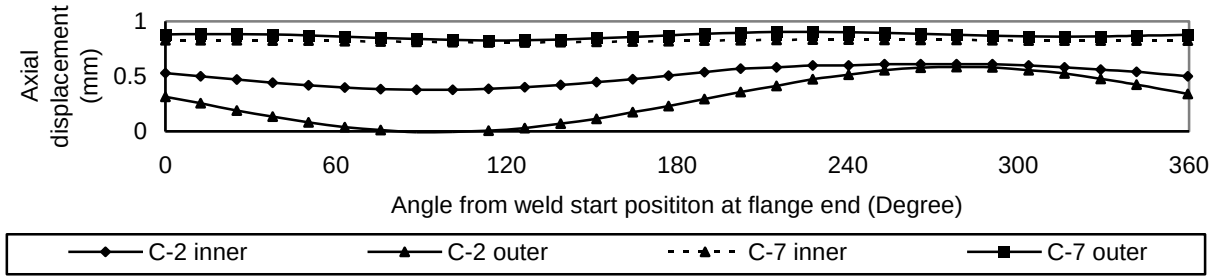

Fig. 8. Axial displacements along inner and outer circumference at flange end

Experimental validation: Residual stresses [Figs. 9a-b] and axial displacements [Fig. 10] are observed in good agreement with the results of Abid et al. in [20] for tack locations at 90 and 270 degrees for root gap of 1.2 mm. In the present work, numbers of elements, are reduced to half along length direction in double ellipsoidal heat source model compared to Siddique's work; this concluded reduced analysis time to almost half. A small difference of 5-10% in stresses results is observed.

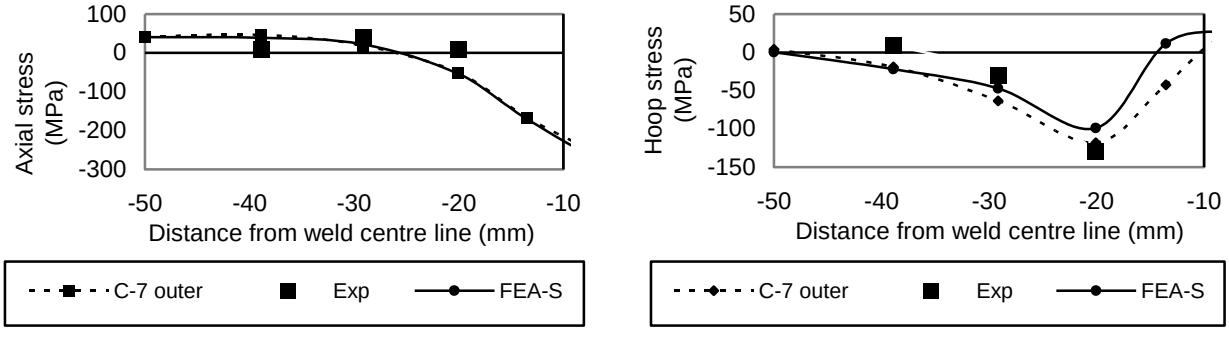

(a) (b)

Fig. 9. Experimental and numerically calculated axial residual stresses on the outer surface of the pipe; (a) Axial stress (b) Hoop stress. (FEA-S=Numerical results by Siddique; EXP=Experimental)

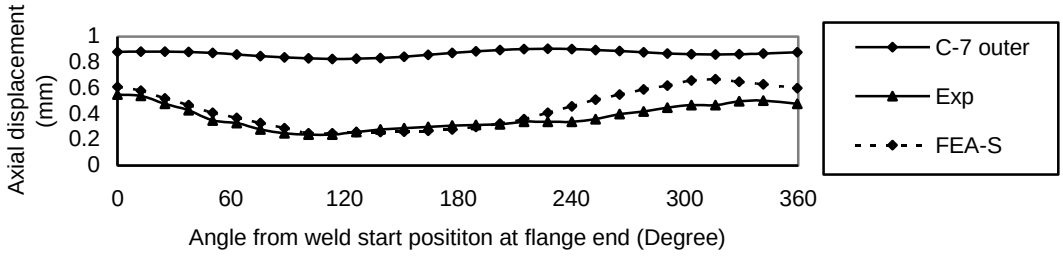

Fig. 10. Comparison of numerical and experimental axial displacement at flange end.
(FEA-S = Numerical results by Siddique; EXP -= Experimental)

d) Effect of pipe thickness on axial and hoop residual stresses

Case studies C-5 and C-6 are conducted for two different thicknesses 8mm and 10 mm of pipe [Fig. 11]. At the pipe side, as thickness increases axial stresses increases, whereas at flange side, inside heat affected zone (approximately), axial stresses increase and away from heat affected zone, axial stresses decrease. With increase in thickness, zone of influence of hoop stresses decreases. At pipe and flange inner diameter, peak stresses increase as pipe thickness increases. At pipe flange outer diameter, peak stresses decrease as pipe thickness increases. Axial displacement at flange inner and outer circumference increases as thickness increases. For a thickness of 10 mm axial displacement occurs in positive direction (elongation) approximately from 90 to 270 degrees (from first tack to second tack) and then in negative direction (compression) occurs from 270 to 90 degrees (from second tack up to first tack), while in case of 8mm thick pipe, no contraction is observed [Fig. 12].

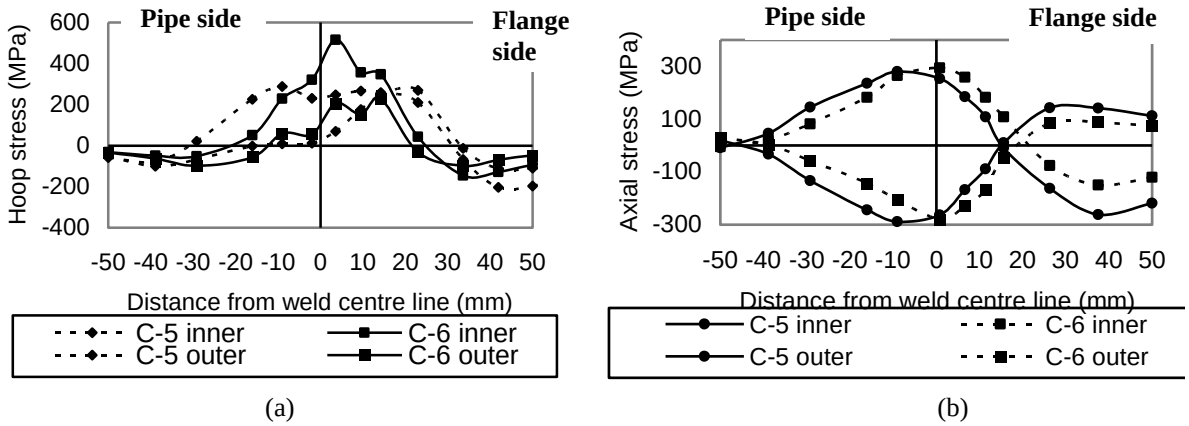

(a) (b)

Fig. 11. Residual stress variation at a section 180 degrees from weld start position: (a) Hoop, (b) Axial

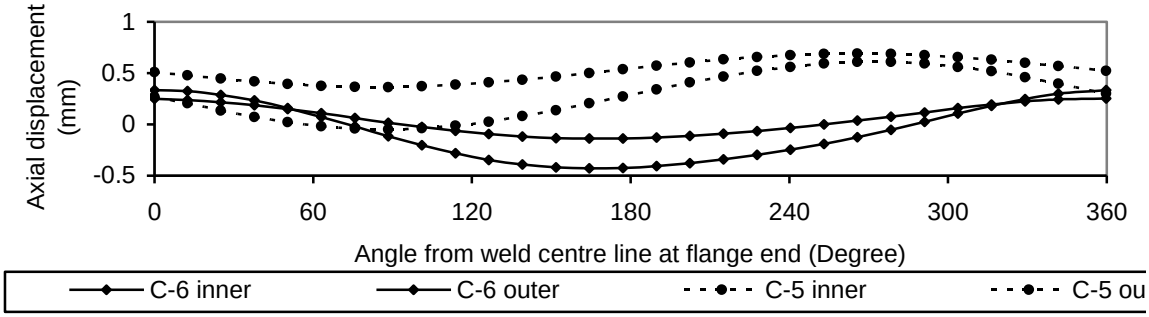

Fig. 12. Axial displacements along inner and outer circumference at flange end

6. CONCLUSION

- Hoop stresses increase at inner and outer diameter of pipe and flange with increase in welding speed, welding current, pipe diameter, and thickness. Their zone of influence also increases with the increases of these parameter except thickness for which zone of influence decreases.
- Axial stresses and their zone of influence increases with increase in welding current, pipe diameter and pipe thickness and decreases with decreases in welding speed.
- Axial displacement increases with increase in welding current and decreases with increases in pipe diameter. Mode of axial displacement changes as pipe thickness increases.
- Overall residual stress variation on the flange side is more prominent due to its dimensional variation, whereas on the pipe side a slight variation in all the cases is observed. Overall axial flange displacement along 360 degrees is quite obvious and is the key finding to avoid gasket crushing, bolt

scatter, bolt relaxation and hub flange yielding due to flange rotation. This ultimately affects sealing of the gasketed flanged pipe joints.

- FE methodology presented may be helpful for developing welding procedures for a range of pipe flange welded joints for controlled residual stresses and deformations for optimized performance during bolt up and operating conditions.

REFERENCES

1. James, F. L. (2000). *The procedure handbook of arc welding*. 14th edition, The James F. Lincoln Arc Welding Foundation, Cleveland, USA.
2. Vaidyanathan, S., Todaro, A. T. & Finnie, I. (1973). Residual stresses due to circumferential welds. *ASME J. Engineering Material and Technology*, pp. 239-242.
3. Rybicki, E. F., Schmueser, D. W., Stonesifer, R. W., Groom, J. J. & Mishler, H. W. (1978). A finite element model for residual stresses and deflections in girth-butt welded pipes. *Journal of Pressure Vessel Technology*. Vol. 100, pp. 256-262.
4. Rybicki, E. F. & Stonesifer, R. B. (1980). An analysis of weld repair residual stresses for an intermediate test vessel. *Journal of Pressure Vessel Technology*. Vol. 102, pp. 323-331.
5. Rybicki, E. F. & McGuire, P. A. (1981). A computational model for improving weld residual stresses in small diameter pipes by induction heating. *Journal of Pressure Vessel Technology*. Vol. 103, pp. 294-299.
6. Rybicki, E. F. & McGuire, P. A. (1982). The effects of induction heating conditions on controlling residual stresses in welded pipes. *Journal of Engineering Materials and Technology*. Vol. 104, pp. 267-273.
7. Jonsson, M. & Josefson, B. L. (1988). Experimentally determined transient and residual stresses in the butt-welded pipes. *Journal of Strain Analysis*. Vol. 23/1, pp. 25-31.
8. Josefson, L., Jonsson, M., Karlsson, L., Karlsson, R., Karlsson, T. & Lindgren, L. E. (1988). Transient and residual stresses in a single-pass butt-welded pipe. ICRS-2, Nancy, France.
9. Lindgren, L. E. & Karlsson, L. (1988). Deformations and stresses in welding of shell structures. *Int. J. Numerical methods in Engineering*. Vol. 25, pp. 635-655.
10. Rosenthal, D. (1946). The theory of moving heat source and its application to metal treatment, *Transactions of ASME*.
11. Karlsson, R. I. & Josefson, B. L. (1990). Three dimensional finite element analysis of temperature and stresses in a single-pass butt-welded pipe. *ASME Journal of Pressure Vessel Technology*. Vol. 112, pp. 76-84.
12. Karlsson, L., Jonsson, M., Lindgren, L. E., Nasstrom, M. & Troive, L. (1989). Residual stresses and deformations in a welded thin-walled pipe. *Proceedings of ASME Pressure Vessel and Piping Conference*, Hawaii. Vol. 173, pp. 7-14.
13. Troive, L., Lindgren, L. E. & Jonsson, M. (1995). Axial collapse load of girth butt-welded pipe. *Proceedings of First International Symposium on Thermal Stresses and Related Topics*, Shizuoka University, Hamamatsu, Japan. pp. 565-568.
14. Troive, L., Näsström, M. & Jonsson, M. (1998). Experimental and numerical study of multi-pass welding process of pipe-flange joint. *ASME Pressure Vessel Technology*. Vol. 120, pp. 244-251.
15. Troive, L. & Jonsson, M. (1994). Numerical and experimental study of residual deformations due to double-j multi-pass butt-welding of a pipe-flange joint. *Proceedings of Annual International Conference on Industry, Engineering and Management Systems*, Cocoa Beach, Florida, USA. pp. 107-114.
16. Teng, T. L. & Chang, P. H. (1997). A study of residual stresses in multi-pass girth-butt welded pipes. *Int. J. Pressure Vessels and Piping*. Vol. 74, pp. 59-70.
17. Rybicki, E. F., McGuire, P. A., Merrick, E. & Wert, E. (1982). The effect of pipe thickness on residual stresses due to girth welds. *Journal of Pressure Vessel Technology*. Vol. 104, pp. 204-209.

18. Rybicki, E. F. & Stonesifer, R. B. (1979). Computation of residual stresses due to multipass welds in piping systems. *Journal of Pressure Vessel Technology*. Vol. 101, pp. 149-154.
19. Siddique, M. (2005). Experimental and finite element investigation of residual stresses and distortion in welded pipe and flange joints. Ph.D Thesis, GIK Institute Topi, KPK, Pakistan.
20. Abid, M. & Siddique, M. (?). Welding simulations for pipe flange joints. VDM Verlag Dr.Muller, UK. ISBN: 978-3-639-21862-6.
21. Abid, M., Siddique, M. & Mufti, R. A. (2005). Prediction of welding distortion and residual stresses in a pipe flange joint using finite element technique. *Modelling and Simulation in Material Science and Engineering*. pp. 455-470.
22. Abid, M. & Siddique, M. (2005). Numerical solution to study the effect of tack weld and root gap on welding deformation and residual stresses of pipe flange joint. *International Journal of Pressure Vessels and Piping*. Vol. 82, pp. 860-871.
23. Siddique, M., Abid, M., Junejo, H. F. & Mufti, R. A. (2005). 3D finite element simulation of welding residual stresses in pipe-flange joints: effect of welding parameters. *Journal of Material Science Forum*. Vol. 490-491, pp. 79-85.
24. Abid, M., Siddique, M. & Mufti, R. A. (2005). Prediction of welding distortions and residual stress in pipe-flange joint using finite element technique. *Journal of Modelling and Simulation in Materials Science and Engineering*. Vol. 13, pp. 455–470.
25. Abid, M. & Siddique, M. (2005). Finite element simulation of tack welds in girth welding of pipe-flange joint. *Journal of Acta Mechanica*. Vol. 178, No.1-2, pp. 53-64.
26. Abid, M. & Siddique, M. (2005). Numerical simulation of the effect of constraints on welding deformations and residual stresses in a pipe-flange joint. *Journal of Modelling and Simulation in Materials Science and Engineering*. Institute of Physics. Vol. 13, pp. 919-933.
27. Siddique, M. & Abid, M. (2005). Numerical simulation of mechanical stress relieving in a multi-pass GTA girth welded pipe-flange joint to reduce IGSCC. *Journal of Modelling and Simulation in Materials Science and Engineering*. Institute of Physics. Vol. 13, pp. 1383-1402.
28. Siddique, M., Abid, M. & Junejo, H. F. (2003). 3-D Finite element simulation of a single pass butt-welded pipe-flange joint. 2nd Intl. *Mechanical Engineering Congress Karachi*, Pakistan. pp. 1-12. Sep 26-28.
29. Siddique, M., Abid, M., Junejo, H. F. & Mufti, R. A. (2004). Three dimensional finite element simulation of welding residual stresses in pipe-flange joints: effect of welding parameters. 7th Intl. *Conference on Residual Stresses in China*. pp. 1-8.
30. Siddique, M., Abid, M. & Mufti, R. A. (2004). Simulation of welding distortions and Residual Stresses in pipe-flange joint using finite element Technique: Comparison of 2D and 3D models. Intl. *Mechanical Engineering Conference*, Kuwait. pp. 674-691.
31. Abid, M. & Siddique, M. (2005). A study of welding deformations and residual stresses in a pipe-flange joint: Effect of constraints. *Tehran Intl. Congress on Manufacturing Engineering*, Tehran, Iran. pp. 1-8.
32. Qarni, M. J. (2008). 3D thermmechanical finite element analysis of residual stresses and distortions due to multi-pass welding in pipe flange joints. MS Thesis. GIK Institute Topi, KPK, Pakistan.
33. Abid, M. & Qarni, M. J. (2010). Numerical investigation of residual stresses and distortions due to multi-pass welding in a pipe flange joint. *Proc. IMechE, Part E: J. Process Mechanical Engineering*, Vol. 224/4. pp. 253-267.
34. Abid, M. & Qarni, M. J. (2009). 3D thermal finite element analysis of single pass girth welded low carbon steel pipe-flange joints. *Turkish J. Eng. Env. Sci*., Vol. 33, pp. 2841-293.
35. Abid, M. & Qarni, M. J. (2009). 3D thermo-mechanical finite element analysis of residual stresses and distortions due to multi-pass welding in pipe flange joints. *3rd National Seminar on Welding Science and Technology*, Islamabad, Pakistan. pp. 1-9.

36. Abid, M. & Sattar U. (2012). Investigation of residual stresses and distortion in welded pipe-flange joint of different classes. *IIUM Engineering Journal*. Vol. 13, No. 2, pp. 145-154.
37. Goldak, J., Bibby, M., Moore, J., House, R. & Patel, B. (1986). Computer of modeling of heat flow in weld. *Metallurgical Transactions B*. Vol. 17B, pp. 587-600.
38. Goldak, J., Chakravarti, A. & Bibby, M. (1984). A new finite element model for heat sources. *Metallurgical Transactions B*., Vol. 15B, pp. 299-305.
39. Andersson, B. A. B. (1978). Thermal stresses in submerged-arc welded joint considering phase transformations. *ASME J. Engineering Material and Technology*. Vol. 100, pp. 356-362.
40. Lindgren, L. E., Runnemalm, H. & Näsström, M. O. (1999). Simulation of multipass welding of a thick plate. *Int. J. Numer. Meth. Eng*., Vol. 44, pp. 1301-1316.
41. British Standard institution, (1989). Circular Flanges for Pipes, Valves and Fittings, BS 1560: Section 3.1.
42. ANSYS Workbench Ver 11, (2008). Engineering Data, Material Library.
43. Lindgren, L. E. & Hedblom, R. (2001). Modeling of addition of filler material in large deformation analysis of multipass welding. *Communication in Numerical Methods in Engineering*. Vol. 17, pp. 647-657.
44. Kelly, F., Joseph, R. & Davis, N. D. (1993). *Wheaton, ASM handbook, welding, brazing and soldering*. Vol. 6, 10th ed. Ohio: ASM International. ISBN 087 1703823.